Structural Effects of Postulated Hydrogen Explosions in Process Piping and Vessels – 20274

Charles H. Keilers, Jr.
Savannah River Remediation

ABSTRACT

At Savannah River Site (SRS), preparations to startup new liquid waste operations and recent advances in understanding thermolytic hydrogen generation have led to several recent studies on the structural effects of postulated hydrogen explosions. This paper reports on seven representative piping and vessel cases that are evaluated for deflagrations, detonations, and deflagration-to-detonation transition (DDT) assuming the initial mixture is stoichiometric hydrogen and air. The evaluations are based on the approach used by the Department of Defense for analyzing structures subjected to accidental explosions and include inelasticity, dynamic structural amplification, and material strain-rate effects. Evaluation criteria consider the potential for repeated explosions causing fatigue but also consider that some degree of permanent plastic deformation is acceptable as long as rupture is prevented. Specific conclusions depend on the assumed pre-ignition pressure. If the pre-ignition pressure is atmospheric and if the components are designed to a code from the American Society of Mechanical Engineers, the components evaluated are expected to plastically deform but not rupture under the explosion scenarios considered.

INTRODUCTION

The Savannah River Site (SRS) Liquid Waste System (LWS) safely stores and treats high-level radioactive waste [1, 2]. The LWS consists of 51 waste storage tanks (eight of which are filled with grout and operationally closed), waste evaporators, and treatment and solidification facilities, such as the Defense Waste Processing Facility (DWPF) and Saltstone Production Facility (SPF). SRS currently has about 130 ML and 9 EBq (244 MCi) of liquid high-level waste (HLW), stored in 43 remaining 4 ML tanks. SRS manages the liquid waste and reduces the associated risks by transfers via piping and by processing in evaporators and vessels. Ultimately, the SRS Defense Waste Processing Facility (DWPF) encapsulates the high-activity waste stream in glass within steel canisters, while the Saltstone Facility immobilizes the low-activity waste stream in grout in Saltstone Disposal Units (SDUs).

Liquid HLW generates hydrogen from radiolytic and thermolytic decomposition; the hydrogen poses an explosion hazard. Unless purged, it may build up to flammable levels – 4 vol% in air or higher. Combustion at low concentrations results in a slow, low-intensity pressure transient – a low-level deflagration – that could injure unprotected personnel but is not structurally damaging. However, at about 12 vol% in constricted geometries, the flame front can accelerate to hundreds of meters-per-second and be capable of deflagration-to-detonation transition (DDT). DDT does not persist but decays to a steady detonation wave, moving at about five times the speed of sound. The resulting pressure transients from either a detonation or DDT are amplified by surface reflections. If initially at stoichiometric concentration (i.e., 29.6 vol% hydrogen in air), the resulting pressure transients are fast but high-intensity, with pressures ranging up to about a hundred atmospheres (10 MPa). Piping and vessels respond dynamically to such transients, which further amplifies the potentially damaging effect compared to a static response to the same pressure. While the likelihood of stoichiometric hydrogen-air explosions is low, the consequences of explosions are such that they are evaluated to ensure safe nuclear operations.

TABLE I. Representative Cases

Case and description	(1) 1-inch Sch 5S	(2) 4-inch Sch 5S	(3) 6-inch Sch 5S	(4) 8-inch Sch 5S	(5) 2-inch Sch 40	(6) head tank wall	(7) pump top cover
Outer diameter, mm (inch)	33.4 (1.31)	114.3 (4.5)	168.3 (6.625)	219.1 (8.625)	60.3 (2.375)	1231.9 (48.5)	508 (20.0)
Reduced thickness, mm (inch)	1.44 (0.06)	1.85 (0.07)	2.42 (0.10)	2.42 (0.10)	3.42 (0.14)	5.56 (0.22)	25.4 (1.0)
Initial abs. pressure, kPa (psia)	101 (14.7)	101 (14.7)	101 (14.7)	101 (14.7)	1200 (180)	101 (14.7)	220 (32)
Differential pressure at yield, MPa (ksi)	21.8 (3.17)	7.92 (1.15)	7.04 (1.02)	5.40 (0.78)	50.3 (7.29)	2.20 (0.32)	6.57 (0.95)
First-mode natural period (msec)	0.019	0.068	0.100	0.131	0.034	0.742	4.2

At SRS, preparations to startup new operations and recent advances in understanding thermolytic hydrogen generation led to several studies since 2015 on the structural effects of postulated hydrogen explosions. These evaluations consider information on deflagrations, detonations, and DDT from multiple sources, particularly the National Fire Protection Association (NFPA) 67, *Guide on Explosion Protection for Gaseous Mixtures in Pipe Systems.*[3] They use methods from the Department of Defense manual for analyzing structures subjected to accidental explosions, [5] and they consider practices from the American Society of Mechanical Engineers (ASME) for evaluating the fitness-for-service of existing systems.[6] Additionally, they use loading histories based on conservatively selected initial pressures and a bounding stoichiometric hydrogen-air mixture. They include the effects of inelasticity, dynamic structural amplification, and the increase in metal yield strength that occurs at high strain rates. This paper describes representative cases, methods, and results.

DISCUSSION

Description of Representative Cases

Table I lists the representative cases. The components evaluated were designed to ASME code; however, explosion effects were outside the scope of the code-based analyses because of their low probability. The material for these cases is stainless steel 304 or 304L. The initial atmosphere is assumed to be stoichiometric at the initial pressure cited in Table I.

Cases (1) to (4) are thin-walled cooling water lines that could collect hydrogen generated by radiolysis. Case (6) is the cooling water system head tank. The concern motivating explosion analyses of these components is that fragmentation missiles could injure nearby personnel or damage nearby nitrogen lines. The nitrogen lines serve a nuclear safety function, in that they are relied upon during off-normal and emergency conditions to inert the head space of radioactive tanks. The head tank has elliptical heads and a capacity of about 1.5 m^3 (i.e., 400 gal). Piping and tank thickness are reduced from nominal to account for manufacturing tolerances. Modeling considered the material to be elastic up to a nominal value for yield [238 MPa (35 ksi)] and then to have no strain-hardening.

Case (7) is for a flat circular plate attached by a fillet weld to the top of a pipe-column. The other end of the pipe-column has a mixing pump, suspended within a 4 ML high-level waste tank. Certain accident scenarios postulate that liquid HLW leaks into the pipe-column and that radiolysis generates hydrogen in the column's vapor space, achieving a pre-ignition pressure of about two atmospheres. If an explosion occurred and the top cover failed, radioactive waste would be ejected onto the tank top and nearby areas. The model included strain-hardening at 2% of Young's modulus after the plate yields. This strain-hardening rate is consistent with realistic material behavior up to about 2% plastic strains. The top cover is evaluated using three different yield strengths; the pressure at yield cited in Table I is based on the intermediate value [310 MPa (45 ksi)] and is provided for perspective. Using a lower yield strength is more limiting for the top cover plate, but a higher yield strength is more limiting for the fillet weld.

Case (5) is an aggressive case, intended to match conditions in a 1972 experiment that plastically deformed but did not rupture a pipe at a blanked end.[10] The initial pressure was 12 atmospheres (162 psig). The hydrogen concentration was about 30% above stoichiometric. The explosion locally expanded the pipe outer radius by about 10 mm (0.4 inches), equivalent to about 34% strain. This analysis used strain-hardening at 1% of Young's modulus and a realistic initial yield strength of 300 MPa (43 ksi).

Deflagrations, Detonations, and Deflagration-to-Detonation Transition (DDT)

Figures 1 and 2 show representative pressure transients for deflagrations, detonations, and DDT. [1, 2] These pressure histories presume that the initial pressure is atmospheric and that the initial composition is stoichiometric hydrogen and air. Explosion analysis often assume the combustion is a constant volume process; therefore, higher initial pressures result in higher final temperatures and explosion pressures.

By definition, a deflagration flame front is moving at less than the speed of sound in the unburnt gas ahead of the flame. For hydrogen in air, initial flame speed is about 3 m/s. The final pressure will be about 0.9 MPa (130 psia) if the initial mixture is stoichiometric at atmospheric pressure (0.1 MPa).[3]

A detonation flame front's speed is greater than the speed of sound in the unburnt gas. For stoichiometric hydrogen and air, the flame front's velocity is about 2,000 m/s, which is about Mach 5, and the final pressure is about 1.7 MPa (250 psia). Reflection can increase a deflagration or detonation peak pressure by a factor of 2 to 2.5, achieving detonation peak pressures of about 4 MPa, as shown in Figure 1.[4]

While a detonation pressure transient is more demanding, direct detonation is much less likely than a deflagration. For a stoichiometric hydrogen-air mixture, the minimum ignition energy for a deflagration (i.e., about 0.02 mJ) is eight orders of magnitude less than the critical energy for direct detonation (i.e., about 5 kJ).[5] Without a higher-energy ignition source, achieving a detonation requires flame acceleration and a deflagration-to-detonation transition, DDT.

[1] NFPA-67, Reference [3], is a useful compendium and the source for most of the information in this section.
[2] Figures 1 and 2 are based on engineering judgment and calculations by Charles M. Vergara and J. Keith Clutter using the CEBAM code. See References [17] and [18] for a CEBAM description.
[3] Reference [3], Table 4.3.2. Reference [4], Sec. 13.3.4.2.(1).
[4] Reference [3], Table 7.3.1 and Section 7.2.2.
[5] References [19]-[20].

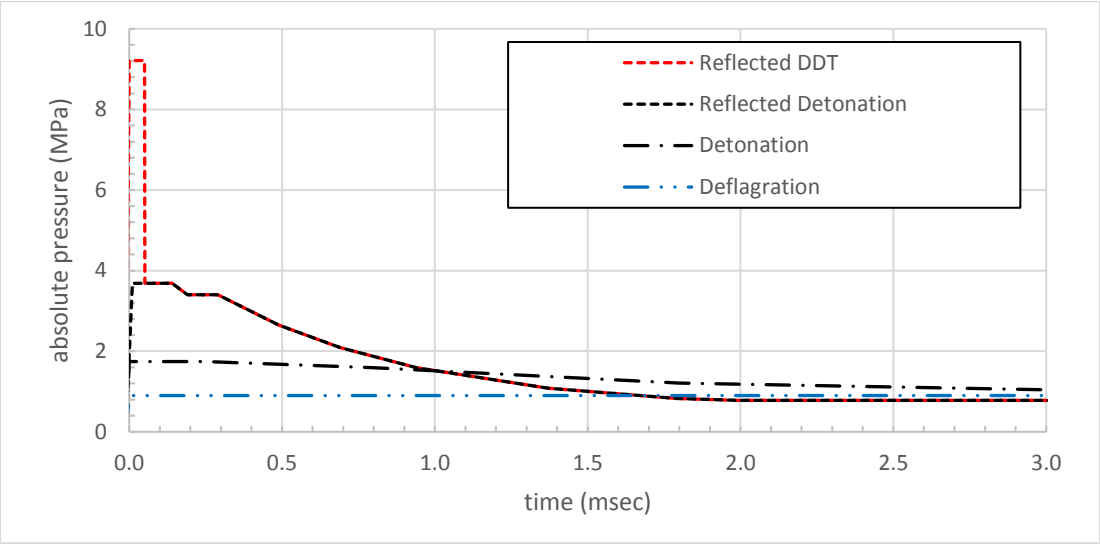

Fig. 1. Representative piping pressure histories from deflagrations and detonations of hydrogen-air stoichiometric mixtures initially at atmospheric pressure.

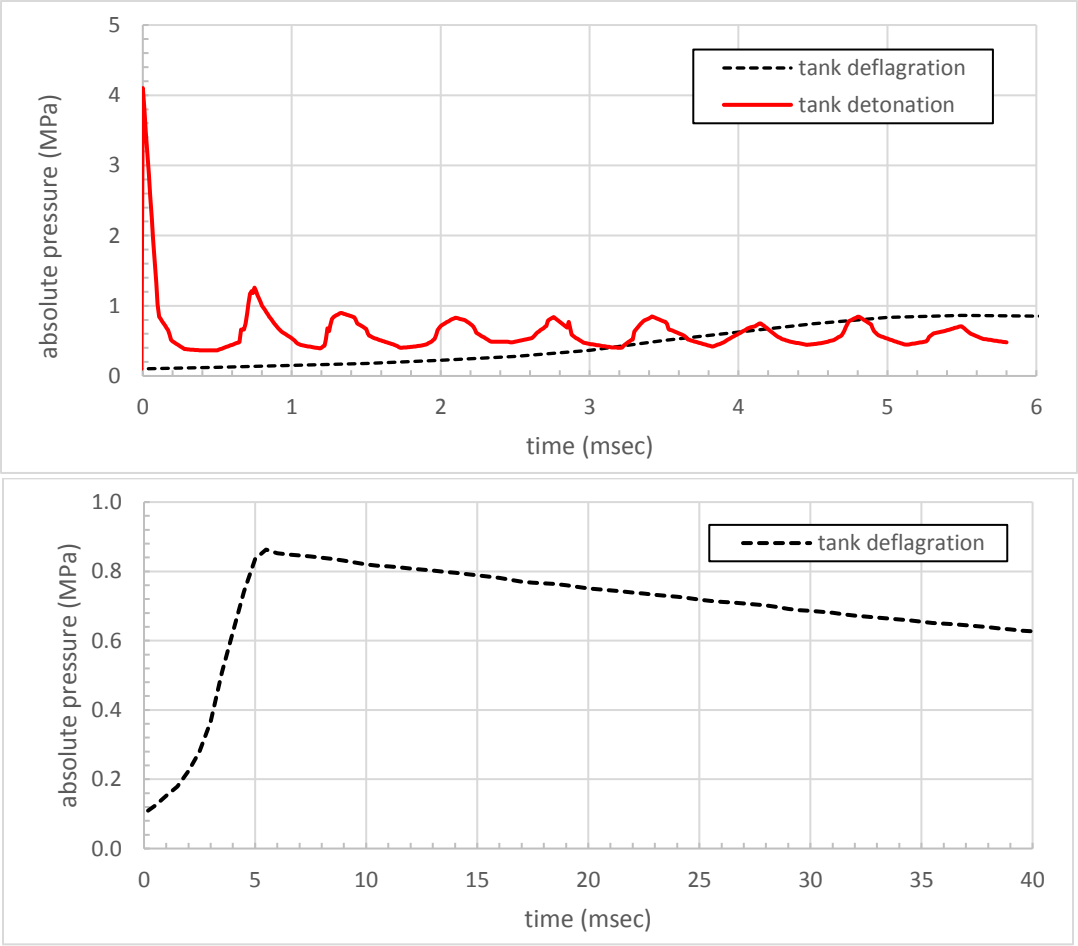

Fig. 2. Representative pressure histories from a tank deflagration and detonation.

DDT is an "over-driven," unstable, highly-localized phenomenon, with peak pressures 1.5 to 4.5 times steady detonation pressures.[6] For unobstructed piping, DDT typically requires 10 to 60 pipe diameters to develop; the over-driven phase persists for one or two pipe diameters before decaying over about ten pipe diameters to a stable detonation wave.[3] More specifically, DDT requires features that promote flame acceleration from a few m/s to hundreds of m/s. The technical literature often refers to flames with speeds in the intermediate range between ~ 600 m/s and ~2,000 m/s as "fast deflagrations" or "quasi-static detonations." Flame fronts in this regime are readily capable of acceleration and DDT.[15] Higher turbulence mixes the hot combustion gases with cooler unburned media and may either accelerate or quench the flame. Obstacles, elbows, surface roughness, or wall reflection increase turbulence that can lead to DDT.

The reflected DDT transient in Figure 1 includes a 50 μsec pulse superimposed on the reflected detonation history. The pressure from a DDT increases if DDT occurs close to a dead end due to unburnt gas "piling up" ahead of the supersonic flame front. The conditional probability of a DDT developing and then occurring close to a dead-end – before it decays to a stable detonation – is much lower than that for a deflagration or a detonation reaching and reflecting off a dead-end. However, assuming a reflected DDT pressure transient is clearly conservative for piping systems. If a piping system can withstand a reflected DDT, then it can also withstand the other more likely but less demanding transients.

For large enclosed spaces, DDT has experimentally occurred for hydrogen concentrations as low as 12% with evenly-spaced obstacles blocking 30% to 50% of the cross-sectional area. [16] Therefore, a large tank with a flammable atmosphere could experience a deflagration, but it is unlikely to have a detonation or DDT without a higher-energy ignition source or features that promote flame acceleration. On the other hand, assuming a detonation from a stoichiometric mixture in a large tank is clearly conservative. If analysis shows the tank can withstand a remotely possible detonation, then it can also withstand a more likely but less demanding deflagration.

Structural Modeling

Evaluations of structural effects from explosions often follow Department of Defense (DOD) practices for analyzing structures to resist accidental explosions,[5] ASME practices for evaluating fitness-for-service for existing applications,[6] and other similar approaches. Some key practices are described below.

Simplified Modeling – SRS has used a variety of structural analysis methods to evaluate explosion effects, ranging from commercial finite element codes to nonlinear, single degree-of-freedom dynamic models. DOD in Reference [5] describes single degree-of-freedom modeling.[7] NFPA-67 cites References [11] and [12] and states that under certain conditions, single degree-of-freedom modeling, based on radial deformation, can be used as an approximation away from pipe end walls and valves. Reference [12] observed that single degree-of-freedom models can reasonably predict residual plastic strains from a reflected detonation at locations equivalent to several pipe diameters away from the reflecting end. The cases discussed here were evaluated with such nonlinear single degree-of-freedom models.[7]

[6] Reference [3], Sections 5.4.4 and 5.4.5.1, and 7.2.3.

[7] The Incremental Linear Acceleration Method was used to perform time integration, Reference [22], Sec. 7.6 and 7.7. Time steps were about 1% of the natural period, which is much smaller than required for numerical stability.

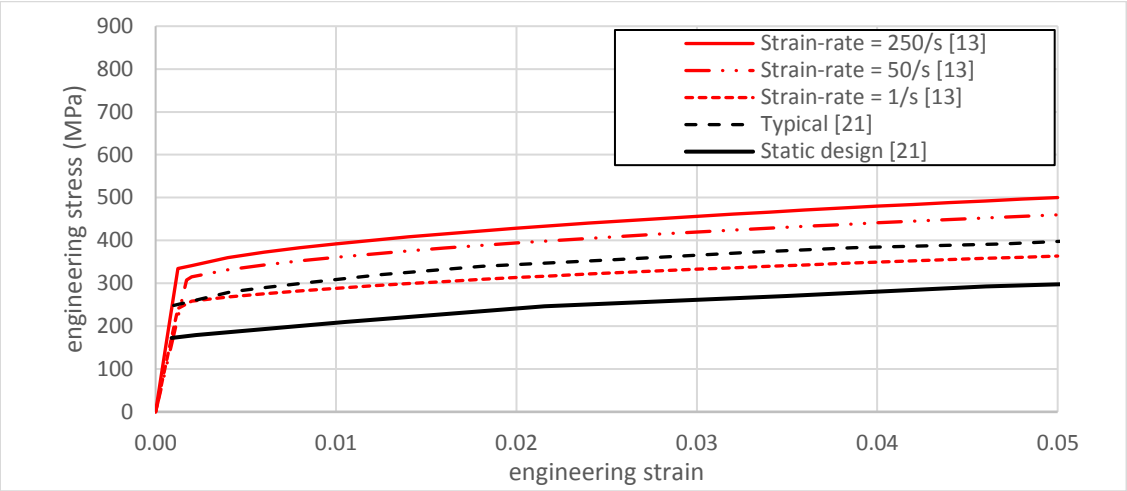

Fig. 3. Engineering stress-strain curves for 304L stainless steel, showing the effect of strain-rate.

Yield Strength Selection – Reference [5] and [6] suggest using nominal yield strength for explosion calculations and fitness-for-service evaluations, respectively. The minimum design yield strength at room temperature for stainless steel 304L is 170 MPa (25 ksi). The expected nominal static yield strength is about 40 percent higher (i.e., 240 MPa, 35 ksi), as shown in Figure 3.[8]

Yield Strength Increase Due to High Strain Rate – Explosions are short intense transients, and the resulting strain-rates increase the yield strength of most metals. Figure 3 illustrates the strain-rate effect, based on the Johnson-Cook material model and representative material properties.[9]

Evaluation Criteria – Evaluation criteria are usually application-specific. Some candidate criteria are:

- Stresses are less than the static or dynamic yield stress (the most restrictive criterion).
- Yielded but stresses are less than a "flow-stress" limit, which is sometimes taken to be the average of yield stress and the ultimate stress.[10]
- Yielded but inelastic strains are less than some value with appropriate margin (e.g., 5% for austenitic stainless steel).
- Yielded but the ratio of maximum displacement to the maximum elastic displacement is less than some value. This ratio is referred to as the *ductility ratio*. For perspective, Reference [5] permits steel ductility ratios up to about 20.[11]

In some cases, a structure needs to remain elastic, for example, if there is a potential for multiple unrecognized explosions leading to fatigue failure. However, in most cases, the high-pressure transient persists for milliseconds, and some inelastic deformation can be tolerated as long as rupture is prevented.[12] In these cases, criteria permitting some degree of yielding are appropriate.

[8] Reference [5], Section 5.13, pg 1447. Reference [6], Annex 2E, Section 2E.2.1, Equation (2E-4).
[9] Reference [5], Section 5-12, pg 1444-1445. Reference [13], Table 5.
[10] Reference [6], Annex 2E, Section 2E.2.2, Equation (2E-5).
[11] Reference [5], Section 5.16.3, pg 1453; Table 5-8, pg 1496.
[12] Reference [4], Section 13.3.4.

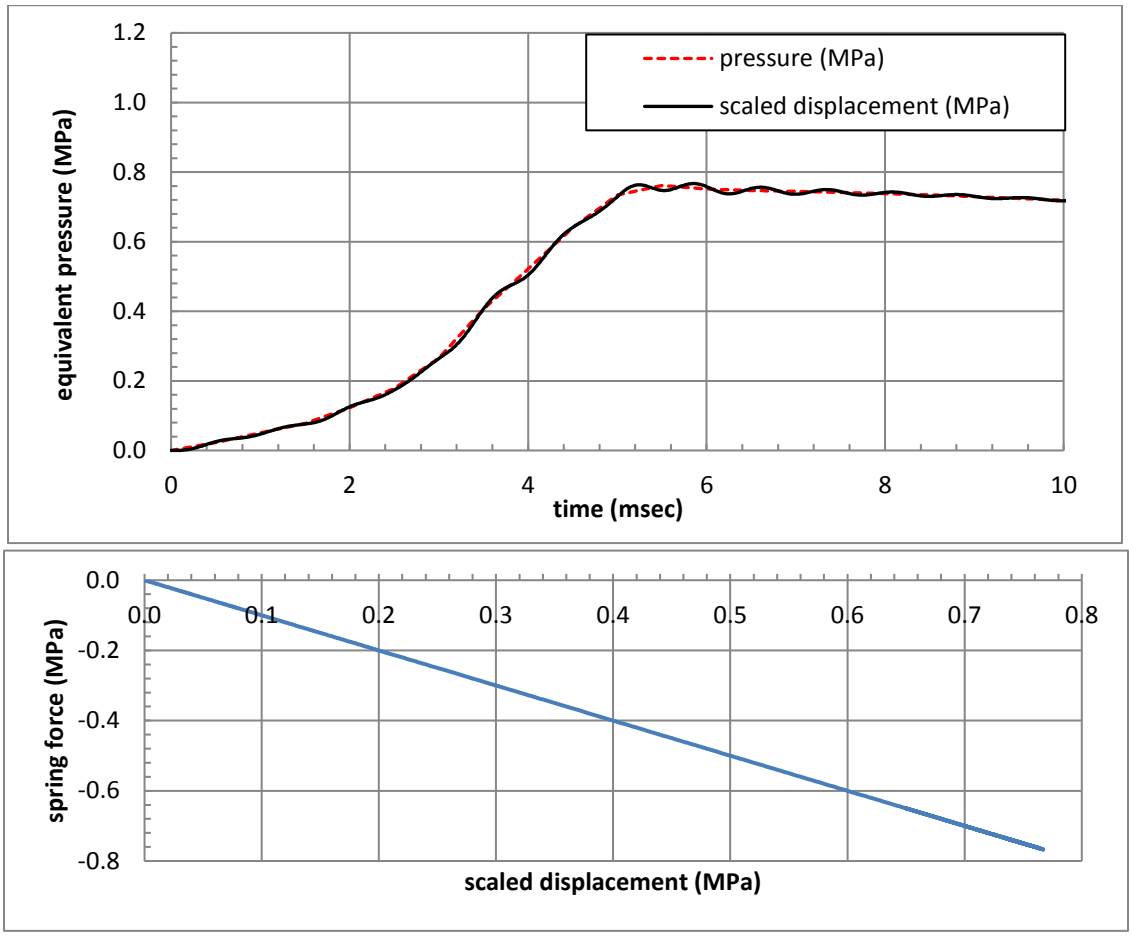

Fig.4. Case (6) – cooling water head tank deflagration response.

Results

Figure 4 shows the results for a deflagration in the cooling water system head tank, Case (6). The upper plot shows the displacement, scaled by the elastic stiffness, and the pressure transient. If the structure is elastic, then the magnitude of the scaled displacement is the same as the reaction or spring force opposing the applied pressure. The lower plot shows the actual spring force vs the scaled displacement. The response is elastic since there is no inelastic offset.

The upper plot also indicates that the deflagration transient is sufficiently slow that the tank wall responds almost as it would to a static load. The scaled displacement is "beating" at the wall's first-mode natural frequency around the applied pressure. The magnitude of response is less than 0.8 MPa, which is well below the pressure at yield from Table I (2.2 MPa).

The Figure 4 quasi-static deflagration response is typical for systems and components designed per ASME code. NFPA 69, Chapter 13, "Deflagration Control by Pressure Containment," has an approach for evaluating such cases that would permit exceeding yield provided there is sufficient margin against the ultimate tensile strength.[13] This is analogous to the "flow-stress" criterion discussed earlier.

[13] Reference [4], Section 13.3.4.

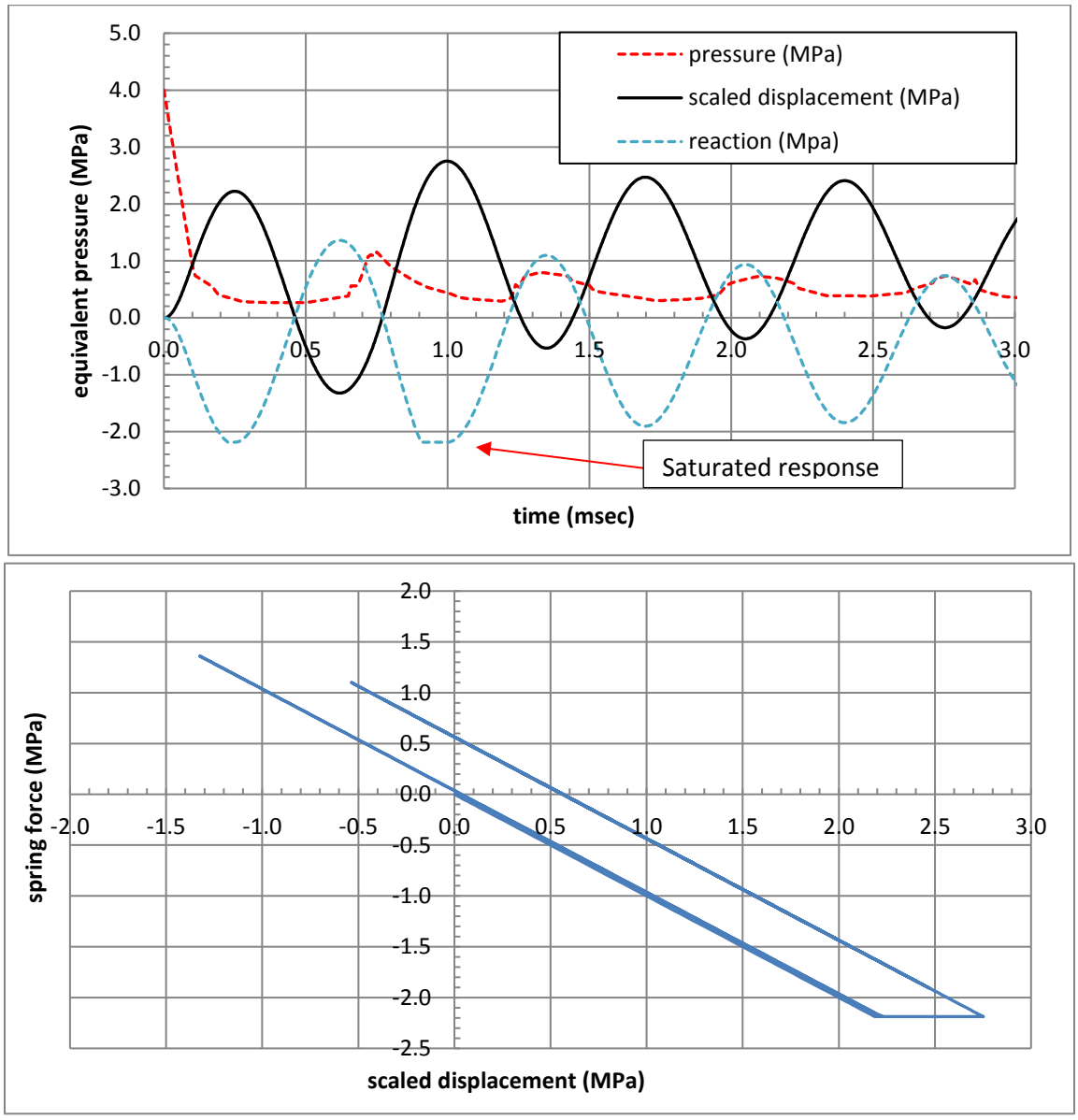

Fig. 5. Case (6) – cooling water head tank detonation response.

Figure 5 shows the head tank's response to the detonation transient. The upper plot now shows not only the pressure transient and scaled displacement but also the opposing reaction force, which is out-of-phase with the displacement. The detonation response is about three times larger than the deflagration response.

During the second cycle, the reaction opposing the applied pressure is sharply "clipped" or saturated at the yield pressure (i.e., at -2.2 MPa) because the model neglects strain-hardening. The wall is assumed to be perfectly plastic following yield. This is evident in the lower plot from the scaled displacement's offset during elastic rebound. In this case, ductility ratio is 1.3, indicating rupture is avoided.

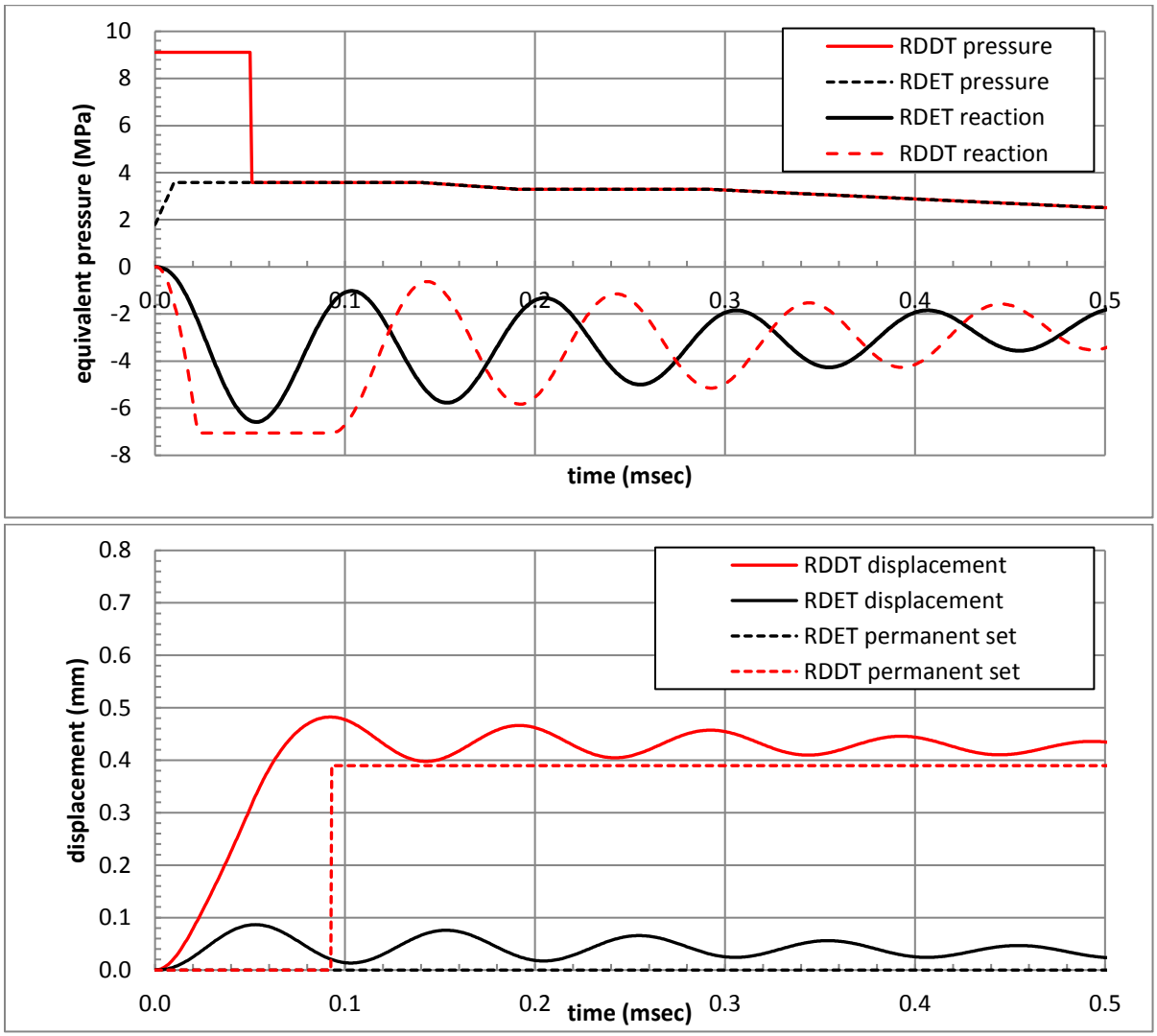

Fig. 6. Case (3) pipe responses to reflected detonation (RDET) and reflected DDT (RDDT).

Figure 6 shows the reflected detonation and reflected DDT responses for the Case (3) cooling water piping (i.e., 6-inch Schedule 5), assuming 5% damping. These are representative of all the piping cases. The upper plot shows the pressure transients and reactions. The lower plot shows the total radial displacements and plastic deformation.

The ductility ratio for reflected detonation is 0.93. The response is elastic and closely resembles the expected elastic response from a step input. In contrast, the reflected DDT reaction is "clipped" at the Table I pressure at yield (-7.04 MPa).

The lower plot shows that reflected DDT causes a permanent offset of about 0.4 mm, and that the pipe displacement is subsequently "beating" about a new permanent radius like a step-input response. The ductility ratio is about 5 and would be considered acceptable under the Reference [5] ductility ratio criterion.

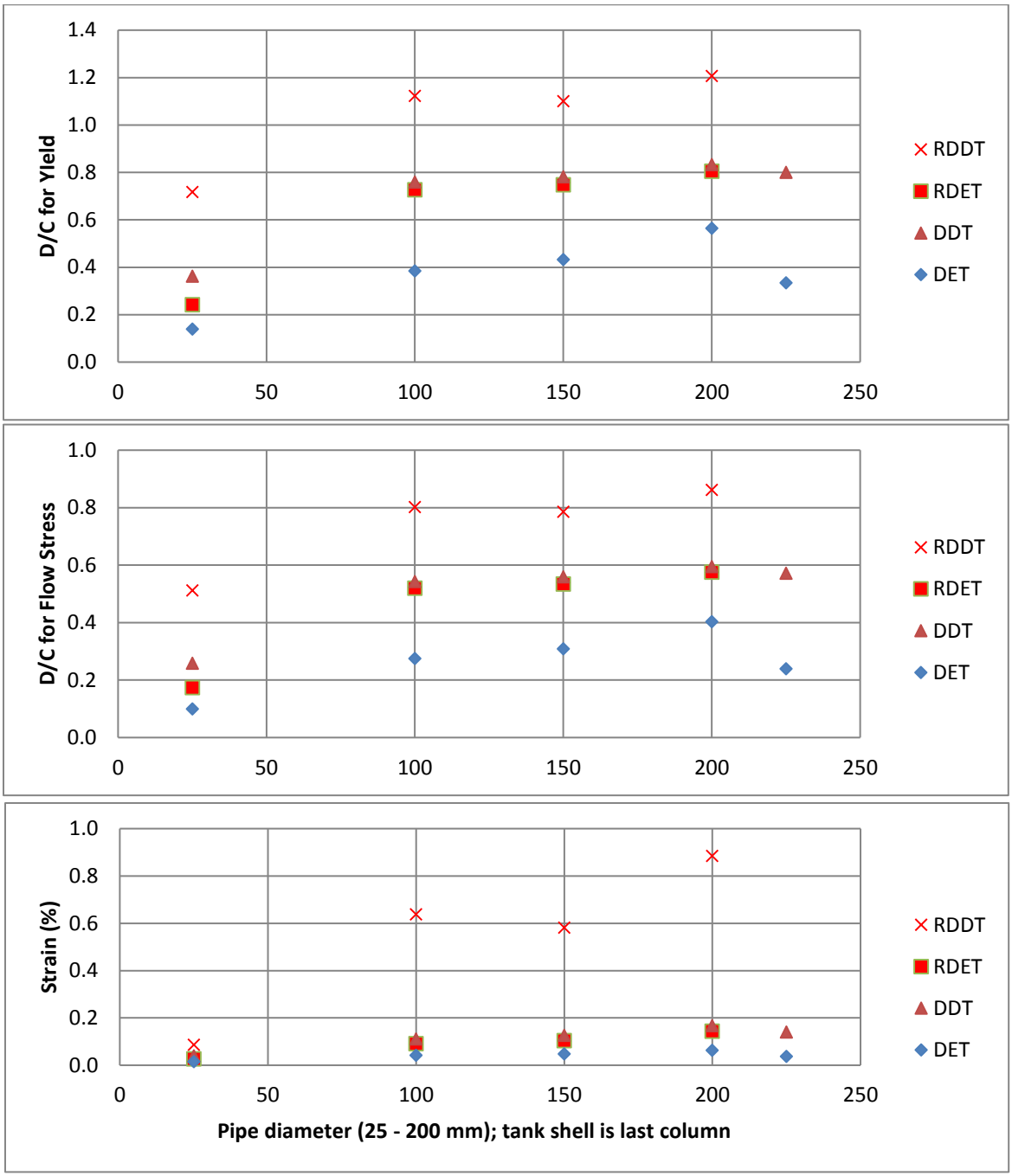

Fig. 7. Demand-to-capacity ratios and strains from cooling pipe and head tank studies.

Figure 7 summaries the results for the cooling pipe and head tank studies, Cases (1) to (4) and (6). Except for reflected DDT, the strains are less than 0.2% and the stresses do not exceed yield [238 MPa (35 ksi)]. In contrast, reflected DDT generates plastic strains, but they are less than 1%, and the stresses are less than the "flow stress" criterion discussed earlier. These results indicate that an explosion due to a stoichiometric hydrogen-air mixture, initially at atmospheric pressure, may plastically deform but will not rupture the cooling water system piping and head tank wall.

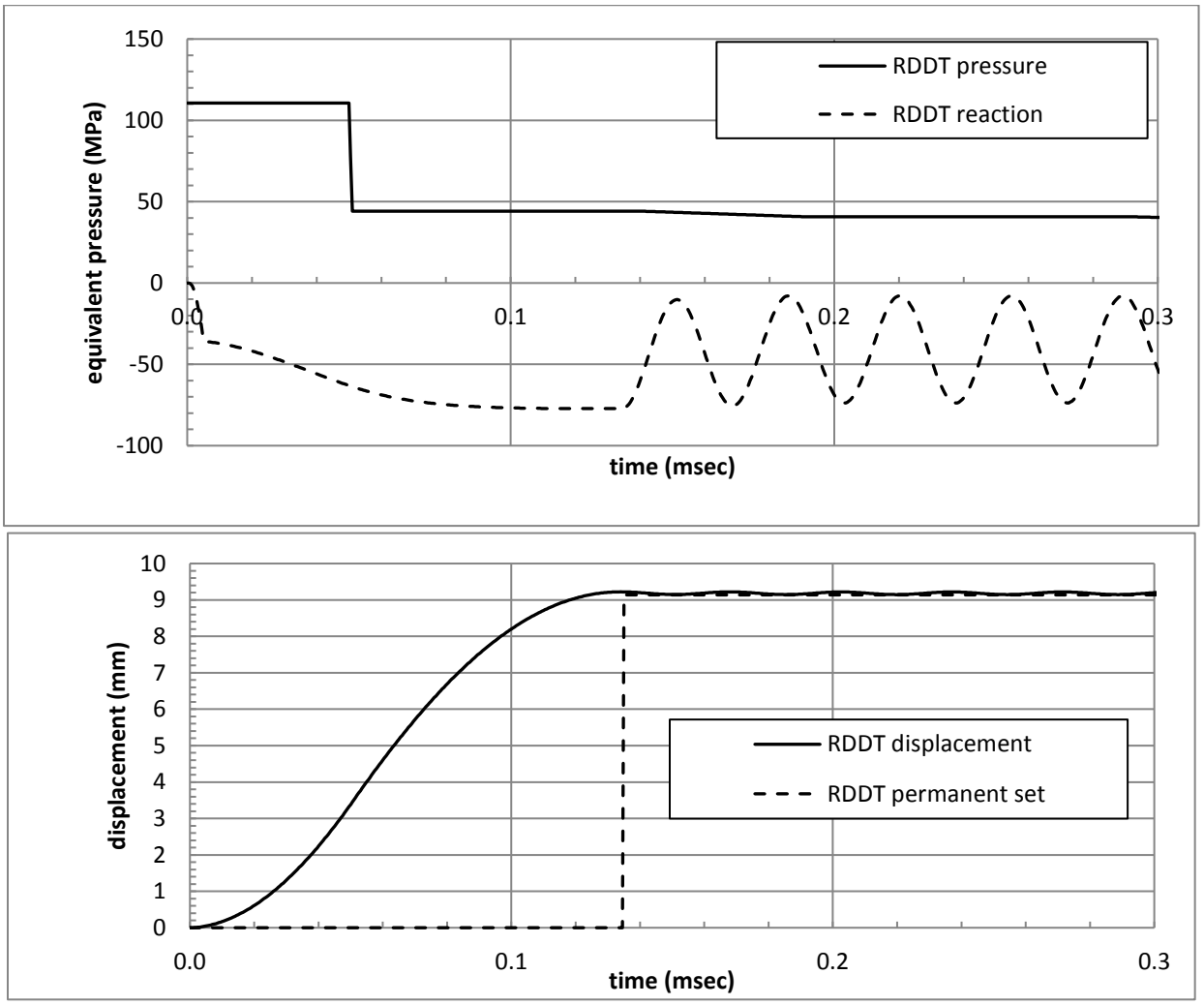

Fig. 8. Case (5) pipe response to a reflected DDT (RDDT) with initial pressure of 12 atmospheres.

Figure 8 shows the response for Case (5) – the aggressive pipe loading case, which has an initial pressure of 12 atmospheres. Strain hardening is 1% of Young's modulus, which matches the expected true stress at a true strain of 40%. This is based on the Johnson-Cook material model and parameters in Reference [13]. Yield strength was also dynamically increased using the Johnson-Cook model. Damping was neglected since plastic deformation predominantly dissipates the energy.

The reaction in the upper plot and the displacement in the lower plot show smoothly developing plastic flow and little dynamics out to about 0.14 msec. During this phase, the pipe is work hardening. Subsequently, the pipe has increased yield strength and is elastically vibrating.

The lower plot shows that the peak calculated displacement is about 9 mm. The true strain is about 0.29. The engineering strain is about 34%. These results are about the same as the experimentally measured values (e.g., peak displacement of about 10 mm). The peak strain is close to the minimum elongation at failure expected for this material (i.e., 35%).[23]

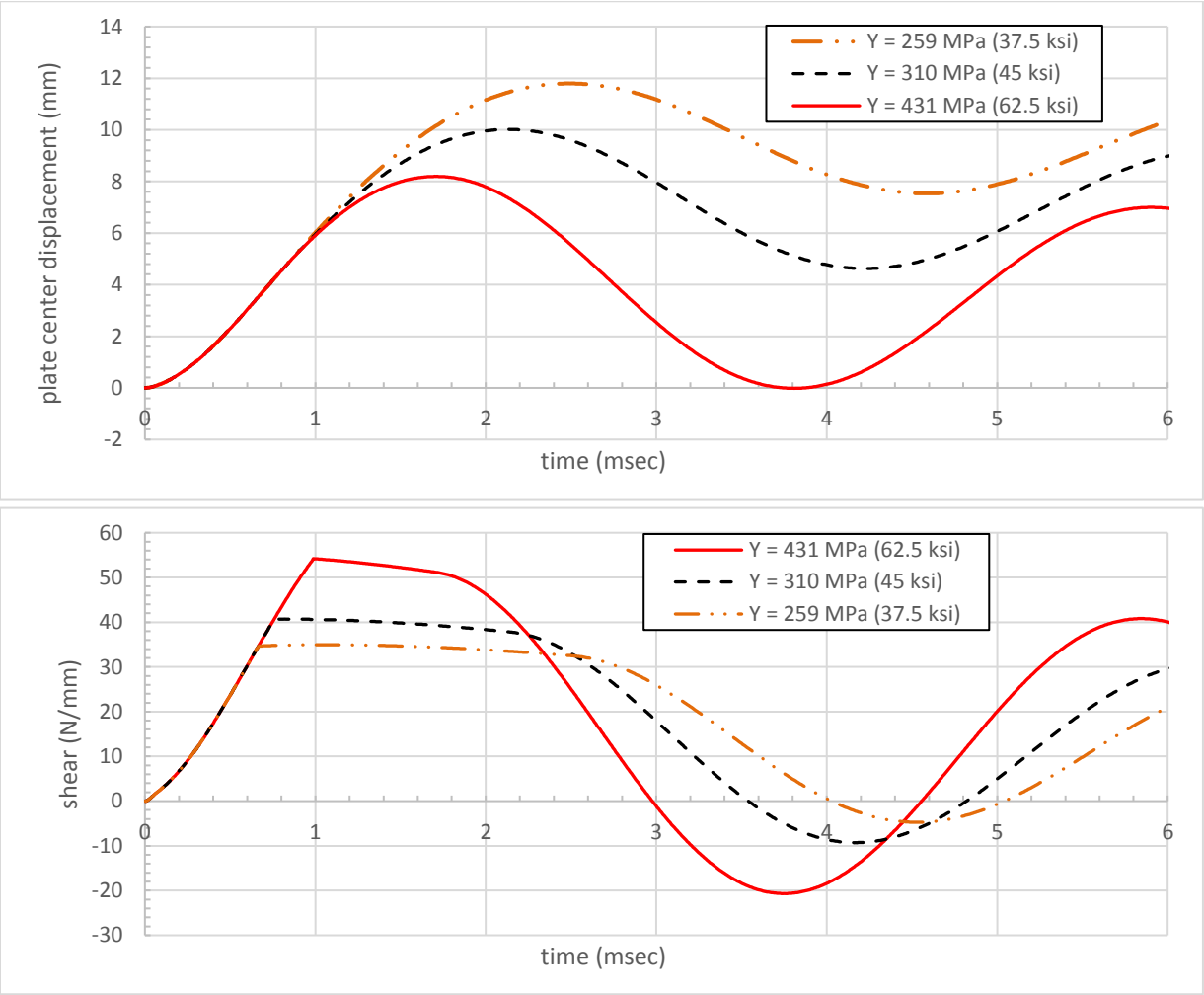

Fig. 9. Case (7) – Responses from reflected DDT for the pump top cover, as a function of yield stress (Y).

Figure 9 shows the responses for the pump top cover from a reflected DDT. The top plot shows the plate's center displacement, while the lower plot shows the shear force in the fillet weld securing the top cover to the pump column. For this case, the pump column is assumed to initially have a stoichiometric mixture at about two atmospheres. This model includes 5% damping, both bending and membrane stiffnesses, and both material and geometric nonlinearity. The post-yield strain-hardening is 2% of Young's modulus. Stiffness also nonlinearly increases as the top cover deflects.[14]

This study assumed a range of different yield strengths to challenge different locations in the top cover. Specifically, the top plot shows that the cover's displacement increases as yield strength decreases. The maximum ductility ratio is about 3.4. The maximum strains occur on the top and bottom surfaces at the center and range up to about 2%. The bottom plot shows the opposite trend, in that shear on the weld increases with plate yield strength. The higher value for yield strength [431 MPa (62.5 ksi)] began to challenge the fillet weld.

[14] Reference [8], Chapter 13, pg 400-404.

CONCLUSIONS

Seven representative piping and vessel cases are evaluated for deflagrations, detonations, and deflagration-to-detonation transition (DDT), assuming the initial mixture is stoichiometric hydrogen and air. The evaluations are based on methodology used by DOD for analyzing structures subjected to accidental explosions, as well as ASME practices for evaluating fitness-for-service of existing applications, and NFPA guidance on evaluating detonations in piping. Inelasticity, dynamic structural amplification, and the material strain-rate effects are included. Evaluation criteria consider the potential for repeated explosions causing fatigue but also consider that some degree of permanent plastic deformation is acceptable as long as rupture is prevented. Specific conclusions depend on the assumed initial pressure. The components evaluated are expected to plastically deform but not rupture under the extreme explosion scenarios considered, given initial atmospheric pressure and ASME code-based design.

REFERENCES

1. D.P. CHEW and B.A. HAMM, *Liquid Waste System Plan*, SRR-LWP-2009-00001, Revision 21, Savannah River Remediation, LLC, 2019. https://www.srs.gov/general/pubs/srr-lw-systemplan.pdf
2. SRR Fact Sheet, "Radioactive Liquid Waste Facilities," August 2019. http://www.srs.gov/general/news/factsheets/srr_rlwf.pdf
3. NFPA-67(2019), *Guide on Explosion Protection for Gaseous Mixtures in Pipe Systems*, National Fire Protection Association.
4. NFPA-69(2019), *Standard on Explosion Prevention Systems*, National Fire Protection Association.
5. DOD UFC 3-340-02, *Structures to Resist the Effects of Accidental Explosions*, December 2008.
6. API 379-1/ASME FFS-1, *Fitness-For-Service*, American Petroleum Institute / American Society of Mechanical Engineers, 2016.
7. BIGGS, J., *Introduction to Structural Dynamics*, McGraw-Hill, 1964.
8. TIMOSHENKO, S. and S. WOINOWSKY-KRIEGER, *Theory of Plates and Shells*, 2nd Edition,
9. McGraw-Hill, 1959.
10. PORTER, J.B., "Analysis of Hydrogen Hazards," Savannah River Laboratory, E.I. DuPont De Nemours & Co., July 1972.
11. SHEPHERD, J.E., "Structural Response of Piping to Internal Gas Detonation," *Journal of Pressure Vessel Technology*, 131(3), June 2009. https://doi.org/10.1115/1.3089497
12. KARNESKY, J., and J. DAMAZO, J.E. SHEPHERD, A. RUSINEK, "Plastic Response of Thin-Walled Tubes to Detonation," PVP2010-25749, *Proceedings of the ASME 2010 Pressure Vessels & Piping Division, July 18-22, 2010, Bellevue, Washington, USA*, 2010.
13. KARNESKY, J. and J. DAMAZO, K. CHOW-YEE, A. RUSINEK, J.E. SHEPHERD, "Plastic Deformation due to Reflected Detonation," *International Journal of Solids and Structures*, 50 (2013) 97-110, 2013. http://dx.doi.org/10.1016/j.ijsolstr.2012.09.003
14. LIGON, T.C. and D.J. GROSS, J.C. MINICHIELLO, "Simplified Methodology for Analysis of Reflected Detonation & DDT, Part 2: Elastic-Plastic Analysis," PVP2014-28464, *Proceedings of the ASME 2014 Pressure Vessels & Piping Conference, PVP2014, July 20-24, 2014, Anaheim, California*, 2014.
15. NEA/CSNI/R(2000)7, *Flame Acceleration and Deflagration-to-Detonation Transition in Nuclear Safety*, OECD Nuclear Energy Agency, https://www.oecd-nea.org/nsd/docs/2000/csni-r2000-7.pdf.

16. DOFOFEEV, S.B., and V.P. SIDOROV, A.E. DVOINISHNIKOV, W. BREITUNG, "Deflagration to Detonation Transition in Large Confined Volume of Lean Hydrogen-Air Mixtures," Combustion and Flame, 104:95-110, 1996. https://doi.org/10.1016/0010-2180(95)00113-1
17. CLUTTER, J.K. and R.T. LUCKRITZ, "Comparison of a Reduced Explosion Model to Blast Curve and Experimental Data," Journal of Hazardous Materials, A79 (2000) 41-61, 2000.
18. LEDIN, H.S., Review of CEBAM Explosion Model, UK Health and Safety Laboratory Report, HSL/2006/112, 2006. http://www.hse.gov.uk/research/hsl_pdf/2006/hsl06112.pdf
19. ONO, R. and T. ODA, "Spark Ignition of Hydrogen-Air Mixture," *Journal of Physics: Conference Series*, 142:012003, 2008. doi:10.1088/1742-6596/142/1/012003.
20. SCHAUER, F.R., etal, "Detonation Initiation of Hydrocarbon-Air Mixtures in a Pulsed Detonation Engine," AFRL-PR-WP-TP-2005-210, 43rd AIAA Aerospace Sciences Meeting, Reno, NV, January 2005. http://www.dtic.mil/dtic/tr/fulltext/u2/a442371.pdf
21. BLANDFORD, R.K. and D.K. MORTON, S.D. SNOW, T.E. RAHL, "Tensile Stress-Strain Results for 304L and 316L Stainless Steel Plate at Temperature," PVP2007-26096, Proceedings of PVP2007, 2007 ASME Pressure Vessels and Piping Division Conference, July 22-26, 2007, San Antonio, Texas. July 2007.
22. CLOUGH, R.W. and J. PENZIEN, *Dynamics of Structures*, 2nd Edition, McGraw-Hill, 1993.
23. ASME SA-312, *Specification for Seamless, Welded, and Heavily Cold Worked Austenitic Stainless Steel Pipes* (from ASME BPVC.II.A-2015).

ACKNOWLEDGEMENTS

The author gratefully acknowledges advice from John R. Neuville, Adeola K. Adediran, and Roy Rothermel during the evaluations discussed in this paper, as well as the benefit and insights gained from extensive relevant work and reports by George Antaki, now with Becht Engineering.